

# Self Contained Plasma Source for Remote and Projected Plasma Generation

D. Carter, D. Hoffman, R. Grilley, and K. Peterson,  
Advanced Energy Industries Inc., Fort Collins, CO

---

## ABSTRACT

Remote plasma sources designed around MF/HF frequencies in the 0.5 to 13 MHz range or at microwave frequencies around 2 GHz have been in use for many years. These sources can offer some unique advantages over *in situ* generated plasmas including high dissociation rates, segregation of ionic/high energy species and a decreased likelihood of damage all while maintaining a high flux density of neutral reactive species. Due to some of the difficulties associated with microwave sources or the limitations in achieving and maintaining H-mode ICP coupling in RF sources, these devices are often designed for specific, narrow range applications, such as chamber cleaning, organic layer ashing or PFC destruction in process effluent. As a result, many existing remote source technologies lack flexibility for use in applications outside their specific design target and so utilization in processes outside their specified purpose is often restricted. This paper introduces a new remote source technology developed to provide high density plasma generation across a broad range of process conditions. The technology utilizes high efficiency VHF electrostatic coupling to provide versatile and robust remote plasma generation. The concept is scalable and adaptable to most any chemistry used for cleaning, etching and even deposition. The unique design allows for operation in multiple modes, ranging from fully remote plasma generation to a projected plasma mode where the active discharge is cast into the processing zone well downstream of the remote source itself. This paper describes some of the important design elements incorporated into these new source devices along with early results illustrating the range in performance exceeding many capabilities of the alternative technologies.

## INTRODUCTION

Remote plasma processing is most commonly used when generation of a plasma or associated high energy species within a processing chamber is undesirable. This may be due to concern for wear on *in-situ* chamber components, incompatible materials in the main chamber or simply the inability of the internal plasma source to produce the desired species with adequate efficiency.

The most common remote plasma application is cleaning dielectric deposits in CVD and PECVD reactors [1, 2]. The approach allows high cleaning efficiencies to be realized without concern for wear of *in-situ* electrodes. Remote source designs have been optimized for this specific task which offers a side benefit of allowing the process chamber's internal structure to be optimized for its intended purpose (deposition).

In recent years, an increasing number of applications gaining advantage from remote plasma generation have begun to emerge. These include low-k dielectric etching and cleaning [3, 4], plasma enhanced atomic layer deposition [5, 6], TCO deposition on flexible substrates [7], surface nitridation and hydrogenation [8, 9], amorphous silicon deposition [10] and both surface preparation and deposition for MOCVD [11, 12].

As trends in device scaling and film stack complexity continue, remote plasma generation is expected to grow in popularity since the approach gives the user extra degrees of freedom for managing parameters such as plasma density, ion to neutral ratios, and ion energies seen in the primary reactor and near to the substrate surface. Especially when sensitive devices are being processed, surface damage and charging can be of utmost importance. Remote plasma generation gives the opportunity to generate an optimized flow of high density radicals without directly exposing the substrate to the high energy plasma used to generate the species of interest.

Despite the many advantages of remote plasma generation, the selection of commercialized, stand-alone devices for an "off the shelf" installation is rather limited. The vast majority of stand-alone source products use one of two methods for coupling power to the discharge, 1) inductive coupling and 2) microwave applicator coupling. Both methods have limitations, the most important being operating range. In particular for inductive sources, efficient operation is only accomplished in the so-called H-mode coupling regime. H-mode coupling is accomplished only under specific flow, pressure and power conditions. Thus, these types of sources are often designed for a specific application having a narrow range of process conditions, often low pressure and high power with limited gas mixtures. Microwave sources tend to be somewhat more flexible, but can also be range limited due to inherent plasma exposure of the applicator and challenges providing necessary cooling to the dielectric components in its construction.

This study looks at an alternative RPS (remote plasma source) technology using a capacitively coupled plasma (CCP) driven with VHF ( $> 40$  MHz) power. Capacitive coupling is generally seen as unfavorable for RPS designs since CCP plasma densities at the traditional frequencies ( $\leq 13.56$  MHz) are low compared to the ICP and microwave alternatives. Similarly, high dc sheath voltages in conventional CCP's create the risk of wall erosion from ion acceleration to electrode surfaces. These issues are largely alleviated by the use of VHF coupling since higher drive frequency provides increased plasma density, decreased sheath thickness and an accompanying drop in dc sheath voltage [13, 14]. These behaviors all suggest that remote, capacitively coupled plasma generation driven at higher frequencies may be a viable alternative with potential advantages compared to ICP and microwave coupled RPS systems.

### VHF RPS DEVICE OVERVIEW

While numerous configurations are possible for capacitively coupling VHF power across a set of electrodes, some lend more favorably to a remote source design. The device evaluated in this study is generally cylindrical in shape with a co-axial electrode arrangement. This design provides advantageous field symmetry in the primary discharge zone and the ability to soften gradients at the boundaries through appropriate and convenient shaping of opposing electrodes.

Figure 1 gives a schematic of a VHF RPS illustrating a pair of opposing CCP electrodes in a cross-sectioned cylindrical form. In this depiction, the chamber and work piece are shown to the right and the plasma source is mounted so as to produce the primary plasma remote from the main chamber. Gas flow is from left to right and carries radical species from the remote source to the work piece accordingly. In the evaluation described herein, a showerhead was optionally placed between the RPS and the work piece to provide uniform flow of reactive species across the surface of the substrate.

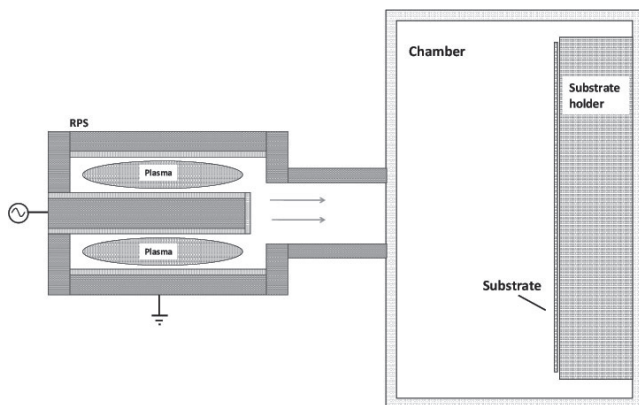


Figure 1: Cross-section of a co-axial CCP RPS mounted remotely to processing chamber (not to scale).

Internal volume of the VHF RPS in this study is approximately two liters with maximum power densities of 5-8 watt/cm<sup>3</sup>. Water cooling is provided to both powered and grounded electrodes to prevent overheating. To avoid chemical attack, all plasma-exposed surfaces within the device are covered with high density, high purity ceramic.

The RPS is powered with a 7 kW maximum power VHF generator. The operating frequency is 60 MHz with sweep frequency capability to aid in impedance matching. The matching circuit is fixed during operation and selectable to allow a wider range of processing conditions.

### EXPERIMENTAL

Since flow delivery manifolds and/or showerheads create pressure differentials, the test system was outfitted with pressure monitoring both within the RPS and at the downstream chamber. During characterization testing, pressures are reported as either RPS (pressure within the RPS unit) or chamber (within the downstream chamber) pressure. The downstream chamber used for all testing had an internal volume of approximately 30 liters and was fitted with a substrate holder capable of handling 300 mm wafers.

Etch rate data were collected on substrates mounted in the downstream chamber. The substrate holder was heated to the appropriate operating temperature and the substrate affixed to the holder with a high conductivity thermal compound to maintain constant temperature during processing runs.

Langmuir probe and optical emission spectroscopy (OES) tests were performed by orienting the RPS on a right angle to the downstream chamber. Access to the output of the source was accomplished by installing a cross-piece flange between the RPS and the chamber serving as the insertion point of the Langmuir probe or for direct (through a quartz viewport) OES sampling of the plasma.

Using these configurations basic plasma properties were measured along with ignition, operating range, spectral output and etch and strip rates in a variety of chemistries. The following sections review highlights of our findings and where possible comparisons to some alternative RPS technologies.

### RESULTS AND DISCUSSION

#### Ignition and Operating Range

Ignition was found to be quite good in the CCP device, in many cases significantly improved over ICP alternatives. For argon and nitrogen, ignition at 200 watts in a fixed frequency and fixed match setting was achieved at RPS pressures up to 20 Torr and 4.4 Torr respectively, independent of flow (up to 10 slm, the limit of the controllers used). In the case of a more electronegative gas, NF<sub>3</sub>, ignition was more challenging, requiring 300 watts to achieve strike at pressures up to 0.9

Torr and flows up to 2.6 liters. The need to achieve “H-mode” operation in an ICP complicates ignition and can narrow the ignition range substantially. By comparison the specified ignition range of a similarly scaled toroidal ICP source is limited to argon only at flows below 1 slm and pressures below 4 Torr.

Operating range of the new VHF RPS is also quite broad. Figure 2a shows the approximate operating range in argon, nitrogen and  $\text{NF}_3$ , Figure 2b shows the VHF RPS nitrogen range compared to that observed with the toroidal ICP RPS and 2c, the same for  $\text{NF}_3$ . As with ignition, the ICP source is limited in operating range by the need to achieve H-mode, high density coupling. At the operating frequencies (0.4 – 4 MHz) for these alternative ICP sources, capacitive coupling does not provide efficient dissociation and further can cause damage to internal components. When in low density, capacitive mode these devices will typically call a fault, thus limiting their operating range. These limitations do not exist

for the VHF RPS since it is intended to operate in the more easily attained CCP mode.

The operating range observed with the VHF RPS suggests versatility not available with alternative source architectures. The ability to operate across a wide range of conditions may allow process optimization with less restriction from the RPS operating space. To gain some insight into how the makeup of the plasma changes in response to the operating conditions, nitrogen OES data were collected at a variety of points across the observed operating window.

Nitrogen plasmas produce a complex mix of ions, atoms and energetic molecular species, and plasma conditions influence the makeup of the mix produced. Figure 3 shows three nitrogen spectra collected at different points within the VHF RPS operating space, all of which are outside the operating window of the ICP RPS. Spectrum a) acquired at 100 watts at

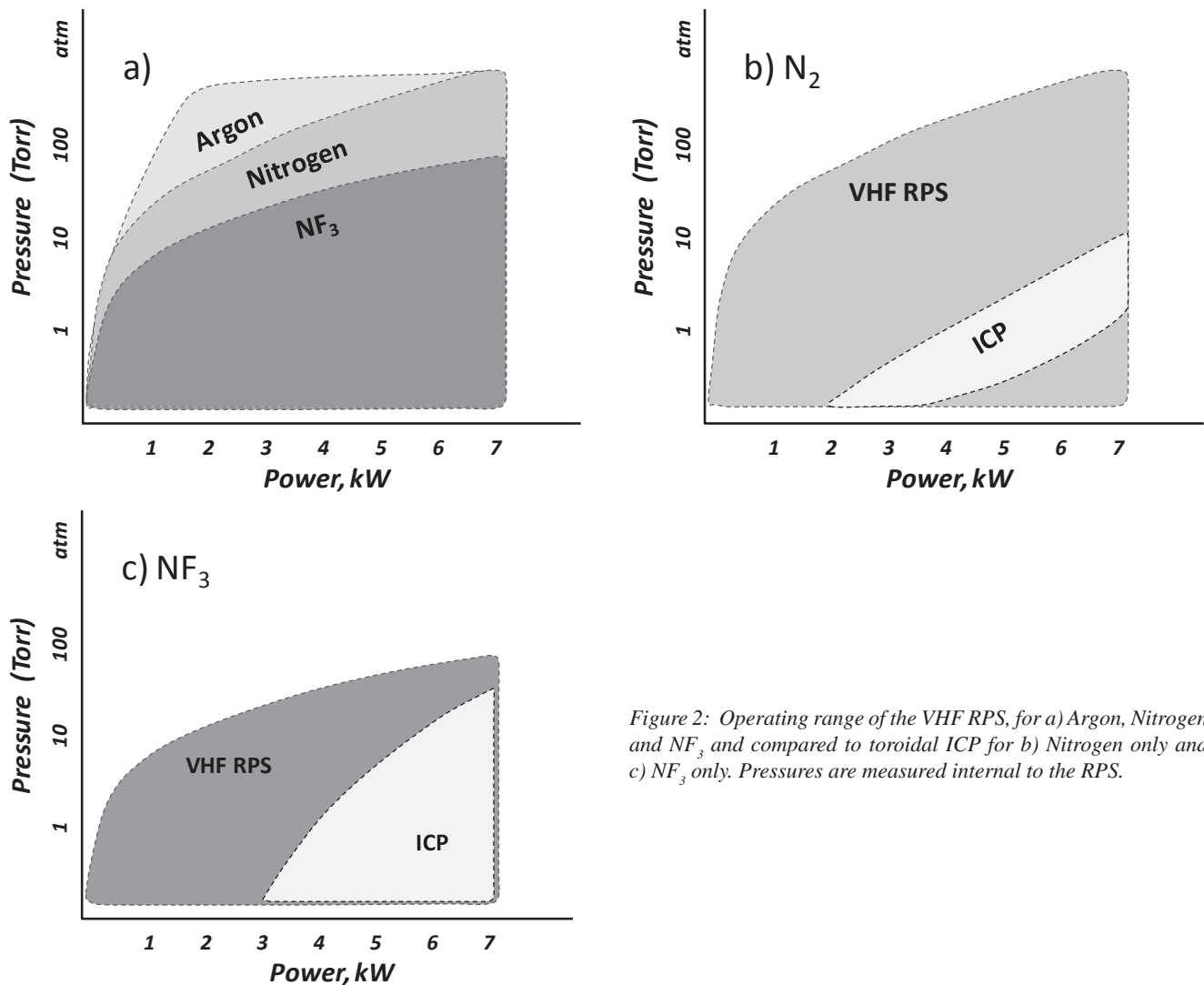


Figure 2: Operating range of the VHF RPS, for a) Argon, Nitrogen and  $\text{NF}_3$  and compared to toroidal ICP for b) Nitrogen only and c)  $\text{NF}_3$  only. Pressures are measured internal to the RPS.

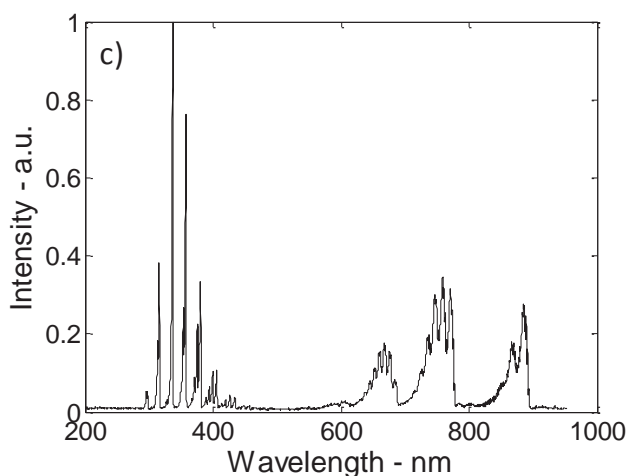
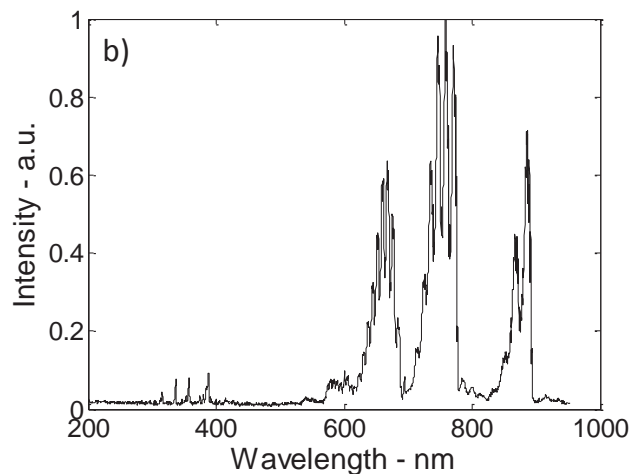
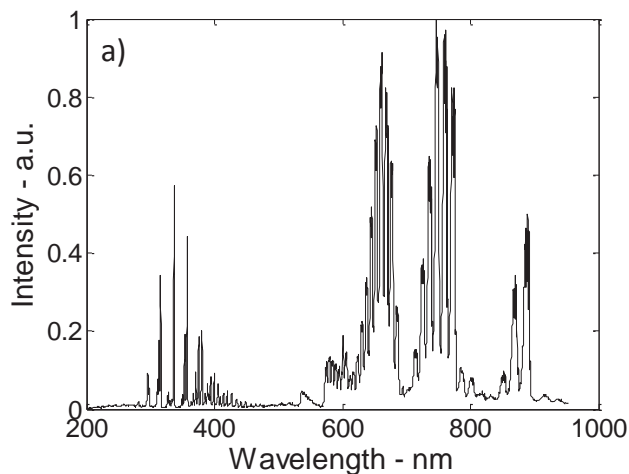


Figure 3: Normalized nitrogen spectra from VHF RPS taken at different operating conditions.

10 mT indicated strong emission from both 1<sup>st</sup> and 2<sup>nd</sup> positive series bands, while spectrum b) at 1000 watts and 28 Torr showed a significant reduction in 2<sup>nd</sup> positive series emission and c) at 2000 watts and 87 Torr showed enhancement of the 2<sup>nd</sup> positive and a reduction in 1<sup>st</sup> positive series bands. For processes particularly sensitive to one or more type species, this flexibility in operation may offer a distinct advantage over RPS alternatives lacking a similar range of operation.

### Langmuir Probe Results

One of the more interesting characteristics of the VHF RPS is an observed “projection” of the plasma beyond the immediate output of the source. While this behavior somewhat contradicts the notion of a “remote” plasma, the implications may include additional performance attributes over traditional RPS devices. To measure the degree of plasma projection a Scientific Systems SmartProbe® Langmuir probe was used to sample argon plasma parameters at and beyond the output of the VHF RPS.

For this test the tip of the Langmuir probe was initially positioned in the plane of the RPS output flange and then translated to a position up to 150 mm downstream. Measurements were made from 100 mT to 10 Torr and from 200 to 1000 watts. Peak densities were seen in the 0.5 to 2 Torr pressure range dependent on power. The maximum density measured was approximately  $2 \times 10^{12} / \text{cm}^3$  at 1.5 Torr and 1000 watts and slightly downstream from the mouth of the source.

As expected from observation, significant density was seen beyond the output of the source. Figure 4 shows density profiles downstream from the source output, plotted by distance from the output flange. The data indicate a considerable amount of plasma escapes the output of the source and is projected downstream. Depending on downstream configuration (how the RPS is mounted to the process chamber, the presence of a showerhead or baffles, etc.) and given the densities measured, this plasma may be maintained by electrostatic fields for a sizeable distance.

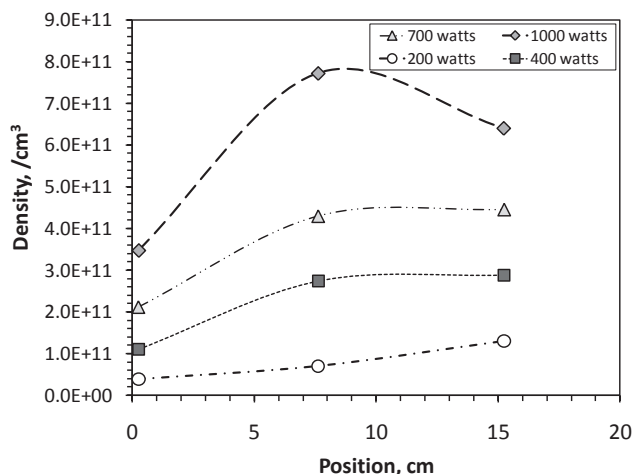


Figure 4: Argon plasma densities measured from the output of the VHF RPS.

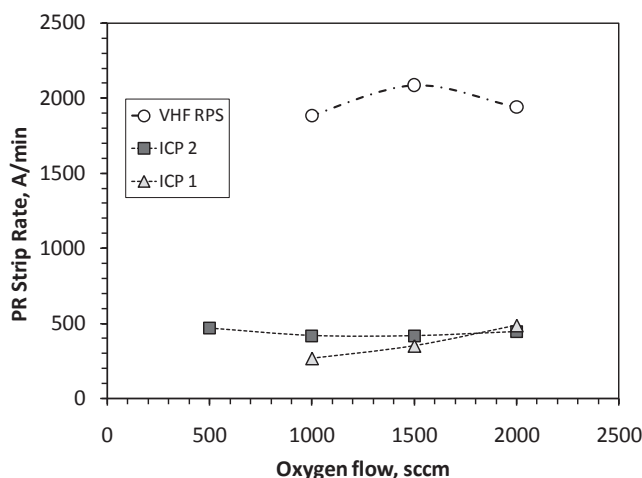


Figure 5: Room temperature photoresist etch rates versus oxygen flow for the three RPS types.

### Etch and Strip Rates

Two of the most common RPS processes are cleaning (or etching) deposits from the walls of deposition chambers and stripping organic films (usually photoresist) from the surface of silicon wafers. To evaluate the performance of the new RPS device for these applications the sample chamber was configured to hold silicon substrates with either TEOS or photoresist coatings. TEOS samples were etched in an  $\text{NF}_3$  plasma, while photoresist was etched in a primarily oxygen plasma. Etch rates were carried out at a constant sample temperature achieved by applying a plasma-inert thermal compound between the silicon wafer and the substrate holder.

A photoresist stripping comparison is shown in Figure 5. Photoresist films were etched using an  $\text{O}_2$ /argon mix at room temperature and 3 kW source power. Two ICP configurations were tested, a linear coil driven unit with a quartz internal structure, and a toroidal device with the standard anodized aluminum internals. The two ICP versions gave similar results, largely independent of flow. Rates measured for the VHF RPS were significantly higher, showing a more than three-fold increase compared to the other RPS systems.

The photoresist tests in Figure 5 were performed without the use of a showerhead. From the Langmuir probe data above, the likely explanation for the increased VHF RPS rate is plasma projection to the substrate surface. This plasma projection results in some plasma exposure on samples. In such a case when no showerhead or other type baffling is present, the VHF RPS appears to act as somewhat of a hybrid source with rates enhanced by direct exposure to the plasma.

Extremely high oxide etch rates are possible using remote plasmas for the generation of fluorine. Figure 6 shows etch rate versus temperature using pure  $\text{NF}_3$  (6 slm flow) at low chamber pressure ( $< 5$  Torr). For this test, no showerhead was present but a baffle plate was inserted in the flow path to prevent plasma projection from the VHF RPS. At room temperature, rates are around 5000 Å/min. The strong temperature dependence of TEOS etching raises the rate to near  $3 \mu\text{m}/\text{min}$  at  $180^\circ\text{C}$ . The trend with temperature very closely follows a second order polynomial with the fitted curve predicting rates exceeding  $5 \mu\text{m}/\text{min}$  at typical deposition temperatures in the  $300^\circ\text{C}$  to  $350^\circ\text{C}$  range.

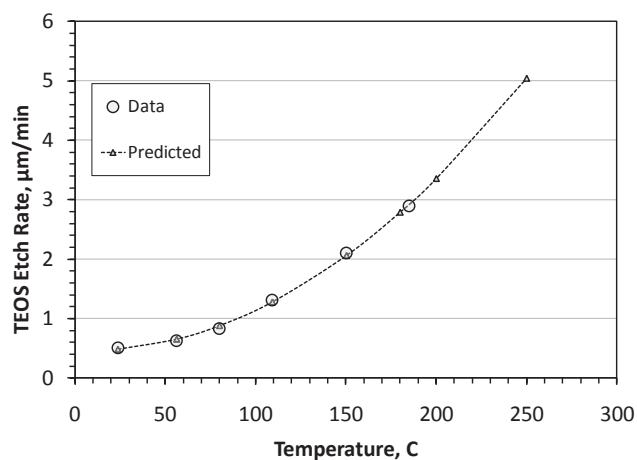


Figure 6: Measured and predicted VHF RPS etch rates for TEOS as a function of temperature in high flow, pure  $\text{NF}_3$ .

The temperature dependence of rates shown in Figure 6 is not unique to the VHF source and similar behavior is seen on alternative source architectures. A more meaningful evaluation of performance compares power and pressure versus rate in a more typical configuration. Figure 7 shows TEOS etch rate versus power for VHF and ICP sources operating in a low  $\text{NF}_3$  flow mixed with argon at 30 Torr (source pressure) through a fine area showerhead. Rates were measured at  $100^\circ\text{C}$  and are noticeably affected by the reduced  $\text{NF}_3$  flow and by accelerated loss mechanisms resulting from the showerhead. The two RPS devices presented similar rates at 5kW (the ICP was not able to maintain plasma below 5kW). At 6kW the VHF RPS peaked at a maximum rate approximately 25% higher than the largely flat trend seen with the ICP source. TEOS etch rate is strongly dependent on fluorine flux to the surface, so these results suggest the ICP RPS reaches its maximum dissociation capability at or near 5 kW, while the VHF RPS sees increasing dissociation, or better immunity to loss mechanisms, to powers up to 6 kW where its trend then became flat.

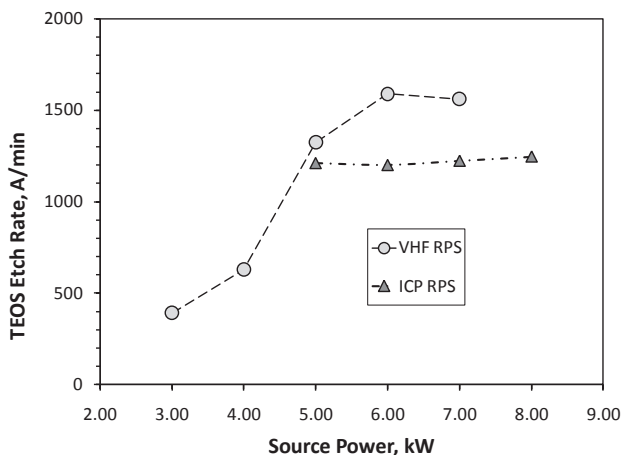


Figure 7: TEOS etch rates versus power in low flow  $\text{NF}_3$  mix for the VHF RPS and toroidal ICP RPS.

TEOS rates versus chamber pressure in high flow, pure  $\text{NF}_3$  are shown in Figure 8. A peak in etch rate for the VHF RPS is seen at approximately 3.5 Torr chamber pressure and at approximately 4 Torr for the ICP source. Maximum rate for the VHF RPS is again somewhat higher compared to the ICP rate, by approximately 10% in this case.

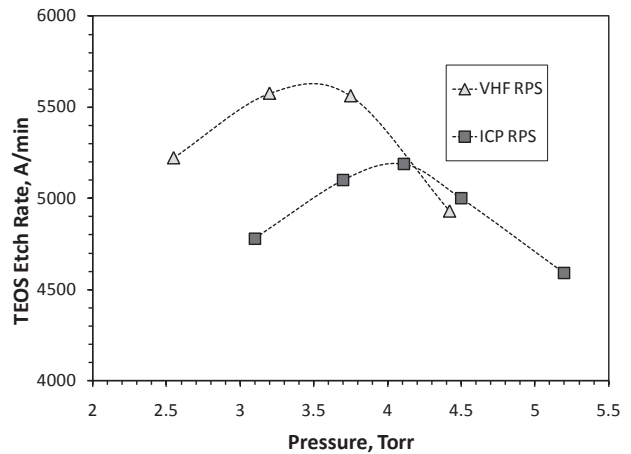


Figure 8: TEOS etch rates versus pressure using pure  $\text{NF}_3$  flow.

## CONCLUSIONS

A new VHF powered capacitively coupled plasma source was evaluated and compared to alternative RPS architectures. The device produced very high plasma densities and appears to offer some significant improvements in ignition and operating range compared to the alternative technologies. Application testing also suggested improved performance in etching and stripping rates on both oxide and photoresist films respectively.

An interesting characteristic of this type of RPS is its ability to project plasma well beyond the confines of the device itself. This plasma projection was confirmed by Langmuir probe measurements and was likely the driving mechanism for a nearly 4x enhancement of room temperature photoresist strip rates. Projection was blocked by the use of a simple baffle plate allowing the RPS to be operated in either remote or projecting modes.

## ACKNOWLEDGEMENTS

The authors wish to thank Victor Brouk and Bill Hattel for their assistance in defining and refining the match circuitry used in the testing conducted in this review.

---

## REFERENCES

1. S. Raoux, T. Tanaka, M. Bhan, H. Ponnekanti, M. Seamons, T. Deacon, L.-Q. Xia, F. Pham, D. Silveti, D. Cheung, K. Fairbairn, A. Jonhson, R. Pearce, and J. Langan, "Remote microwave plasma source for cleaning chemical vapor deposition chambers: Technology for reducing global warming gas emissions," *J. Vac. Sci. Technol. B* 17 (2), (1999).
2. S. Gangoli, A. Johnson, A. Fridman, R. Pearce, "Production and transport chemistry of atomic fluorine in remote plasma source and cylindrical reaction chamber," *A F Gutsol and A Dolgopolsky, J. Phys. D: Appl. Phys.* 40, 5140–5154 (2007).
3. Y. Yun, S. Park, D. Kim, N. Lee, C. Choi, K. Kim, G. Bae, "Effects of various additive gases on chemical dry etching rate enhancement of low-k SiOCH layer in F2/Ar remote plasmas," *Thin Solid Films*, 516 (11), 3549-3553, (2008).
4. M. Kuo, X. Huaa, G. Oehrlein, A. Ali, P. Jiang, P. Lazzeri, and M. Anderle, "Influence of C4F8/Ar-based etching and H2-based remote plasma ashing processes on ultralow k materials modifications," *J. Vac. Sci. Technol. B* 28 284 (2010).
5. S. Heil, J. van Hemmen<sup>1</sup>, C. Hodson, N. Singh, J. Klootwijk, F. Roozeboom, M. van de Sanden, and W. Kessels, "Deposition of TiN and HfO<sub>2</sub> in a commercial 200 mm remote plasma atomic layer deposition reactor," *J. Vac. Sci. Technol. A* 25 1357 (2007).
6. J. Kim, S. Seo, D. Kim, H. Jeon, and Y. Kim, "Remote plasma enhanced atomic layer deposition of TiN thin films using metalorganic precursor," *J. Vac. Sci. Technol. A* 22 8 (2004).
7. S. Wakeham, M. Thwaites, B. Holton, C. Tsakonas, W. Cranton, D. Koutsogeorgis, and R. Ranson, "Low temperature remote plasma sputtering of indium tin oxide for flexible display applications," *Thin Solid Films*, 518 (4), 1355-1358, (2009).
8. T. Ohachi, N. Yamabe, H. Shimomura, T. Shimamura, O. Ariyada, and M. Wada, "Measurement of nitrogen atomic flux for RF-MBE growth of GaN and AlN on Si substrates," *Journal of Crystal Growth* 311 (2009) 2987–2991.
9. S. Honda, T. Mates, K. Knizek, M. Ledinsky, A. Fejfar, J. Kocka, T. Yamazaki, Y. Uraoka, and T. Fuyuki, "Hydrogenation of polycrystalline silicon thin films," *Thin Solid Films*, 501, (1-2), 144-148 (2006).
10. M. Jeon, S. Yoshida, and K. Kamisako, "Hydrogenated amorphous silicon film as intrinsic passivation layer deposited at various temperatures using RF remote-PECVD technique," *Current Applied Physics*, 10, 2/1 (2010).
11. G. Bruno, M. Losurdo, M. Giangregorio, P. Capezzuto, A. Brown, T. Kim, S. Choi, "Real time ellipsometry for monitoring plasma-assisted epitaxial growth of GaN," *App. Surf. Sci.*, 253 (1), 219-223 (2006).
12. M. Giangregorio, M. Losurdo, P. Capezzuto, and G. Bruno, "Role of plasma activation in tailoring the nanostructure of multifunctional oxides thin films," *Appl. Surf. Sci.*, 255, 10 (1) 5396-5400 (2009).
13. V. Vahedi, C. Birdsall, M. Lieberman, G. DiPeso, and T. Rognlien, "Verification of frequency scaling laws for capacitive radio-frequency discharges using two-dimensional simulations," *Phys. Fluids B* 5 (7) (1993).
14. S. Rauf, and M. Kushner "Nonlinear Dynamics of Radio Frequency Plasma Processing Reactors Powered by Multifrequency Sources," *IEEE Transactions on plasma science*, 27, 5 (1999).